Insight into the thermal decomposition of kaolinite intercalated with potassium acetate: An evolved gas analysis

Hongfei Cheng [a,b,c], Kuo Li [a], Qinfu Liu [a], Shuai Zhang [a], Xiaoguang Li [a], Ray L. Frost [c•]

[a] *School of Geoscience and Surveying Engineering, China University of Mining & Technology, Beijing 100083, P.R. China*

[b] *State Key Laboratory of Coal Resources and Safe Mining, China University of Mining & Technology, Beijing 100083, P.R. China*

[c] *School of Chemistry, Physics and Mechanical Engineering, Science and Engineering Faculty, Queensland University of Technology, 2 George Street, GPO Box 2434, Brisbane, Queensland 4001, Australia*

Abstract The thermal decomposition process of kaolinite-potassium acetate intercalation complex has been studied using simultaneous thermogravimetry coupled with Fourier-transform infrared spectroscopy and mass spectrometry (TG-FTIR-MS). The results showed that the thermal decomposition of the complex took place in four temperature ranges, namely 50-100, 260-320, 320-550 and 650-780 °C. The maximal mass losses rate for the thermal decomposition of the kaolinite-potassium acetate intercalation complex were observed at 81, 296, 378, 411, 486 and 733 °C which were attributed to (a) loss of the adsorbed water (b) thermal decomposition of surface-adsorbed potassium acetate (KAc) (c) the loss of the water coordinated to potassium acetate in the intercalated kaolinite (d) the thermal decomposition of intercalated KAc in the interlayer of kaolinite and the removal of inner surface hydroxyls (e) the loss of the inner hydroxyls and (f) the thermal decomposition of carbonate derived from the decomposition of KAc. The thermal decomposition of intercalated potassium acetate started in the range 320-550 °C accompanied by the release of water, acetone, carbon dioxide and acetic acid. The identification of pyrolysis fragment ions provided insight into the thermal decomposition mechanism. The results showed that the main decomposition fragment ions of the kaolinite-KAc intercalation complex were water, acetone, carbon dioxide and acetic acid. TG-FTIR-MS was demonstrated to be a powerful tool for the investigation of kaolinite intercalation complexes. It delivers a detailed insight into the thermal decomposition processes of the kaolinite intercalation complexes characterized by mass loss and the evolved gases.

Keywords kaolinite, potassium acetate, intercalation complex, thermal decomposition, evolved gas

• Corresponding authors. Fax:+86 10 62331825 (Q. Liu) , +61 7 3138 2407(R. L. Frost)
E-mail addresses: lqf@cumtb.edu.cn (Q. Liu), r.frost@qut.edu.au (R. L. Frost)

Introduction

Intercalation reaction of inorganic layered materials has been well-known as a method for the preparation of inorganic-organic multilayer nanocomposites, which have drawn increasing attention in recent ten years [1-9]. The preparation and characterization of kaolinite intercalation composite nanoparticles were discussed in a great number of publications [10-13]. Kaolinite intercalation composites are widely used in the fabrication of paper, paints and inks, rubber and plastic, fiberglass, cracking catalysts, cosmetics, medicines, etc. [14-16]. It is useful because of their high specific surface area, chemical and physical stability, and surface structural properties. Many researchers have focused on the organic intercalation. They used organic molecular to intercalate the layer of kaolinite and improve its specific area and reduce the particle size. The intercalation can separate the particles of kaolinite into thin platelets, and the characteristics of the kaolinite are remarkably improved. Therefore, intercalation is an effective way to construct high performance inorganic-organic nanocomposite.

Various inorganic and organic species can be used in the intercalation of kaolinite, such as formamide [17, 18], dimethylsulfoxide [19], urea [20], potassium acetate [21], aniline [22] and hydrazine [23]. Potassium acetate (KAc) has been shown to readily intercalate within the kaolinite structure [24, 25]. Also of significant interest regarding the kaolinite-KAc complex is its thermal behavior and decomposition [24, 26]. This is because heating treatment of intercalated kaolinite is necessary for its further application, especially in the field of plastic and rubber industry. In order to elucidate

the thermal decomposition processes of kaolinite-KAc intercalation complex, here we present our study on identification and tracking of evolving gaseous species from the intercalation complex pyrolysis using simultaneous thermogravimetry coupled with Fourier-transform infrared spectroscopy and mass spectrometry (TG-FTIR-MS). TG-FTIR-MS a powerful method has been used in previous studies to measure evolved gases during the thermal treatment of various substances [27-33]. The components of released gaseous mixtures have been monitored and identified mostly on the basis of their Fourier-transform infrared spectroscopy (FTIR) and mass spectrometry (MS). Evolution curves obtained in flowing air by TG-MS-FTIR methods are compared in details [34-36]. This method offers the potential for the non-destructive, simultaneous, real-time measurement of multiple gas phase compounds in complex mixture.

This paper, based on authors' previous work [6, 37], reports the thermal decomposition of kaolinite-KAc intercalation complex using TG-FTIR-MS. The purpose of the present study is to make clear the thermal decomposition processes of kaolinite-KAc intercalation complex and provide new insight regarding the thermal decomposition mechanism of the kaolinite intercalation complex.

Experimental

Materials

The sample used in this study was the natural pure kaolinite from Hebei Zhangjiakou in China with an average grain size of 45 μm. The particle size of this

sample was measured with the Malvern Mastersizer 2000. Its chemical composition in mass% is SiO_2 44.64, Al_2O_3 38.05, Fe_2O_3 0.22, MgO 0.06, CaO 0.12, Na_2O 0.27, K_2O 0.08, TiO_2 1.14, P_2O_5 0.13, MnO 0.002, loss on ignition 15.06. The major mineral constituent is well ordered kaolinite (95 mass %) with a Hinckley index of 1.31. The potassium acetate (A. R) was purchased from Beijing Chemical Reagents Company, China.

Intercalation reaction

The kaolinite-KAc intercalation complex was prepared by immersing 10 g of kaolinite in 20 mL of KAc solution at a mass percentage concentration of 30 %. The sample was stirred for 10 minutes at room temperature. The complex after aging for 24 h was allowed to dry at room temperature before the X-ray diffraction (XRD) and TG-MS-FTIR analysis.

Characterization

X-ray diffraction (XRD)

The XRD patterns of the prepared intercalation complex samples were performed using a Rigaku D/max 2500PC x-ray diffractometer with Cu (λ=1.54178 Å) irradiation at the scanning rate of 2 °/min in the 2θ range of 2.6-60 °, operating at 40 kV and 150 mA.

In situ TG-MS-FTIR

The TG-FTIR-MS analysis was performed using simultaneous thermogravimetry (Netzsch Sta 449 C) coupled with FTIR (Bruker Tensor 27) and mass spectrometry

(ThermoStar, Pfeiffer Vacuum). About 10 mg of the sample was heated under nitrogen flow rate of 60 mL min^{-1} and a heating rate of 10 °C min^{-1} from 30 °C to 1200 °C. The capillary connections for gas transportation between the apparatuses were set at 200 °C to allow the decomposition products in a gaseous state. The gas ionization was performed at 100 eV. The m/z was carried out from 1 to 100 amu to determine which m/Z has to be followed during the TG experiments. The ion curves close to the noise level were omitted. Finally, only the intensities of 10 selected ions (m/Z =15, 16, 17, 18, 32, 43, 44, 45, 58 and 60) were monitored with the thermogravimetric parameters. The bottom of the thermoanalyser was heated to about 200 °C to eliminate cold points in the connecting line. The FTIR spectra were collected at a resolution of 4 cm^{-1}, and 200 scans were co-added per spectrum. The literature on the thermal decomposition of kaolinite and its intercalation complexes shows that the most important gaseous products evolved during devolatilisation are CO_2, H_2O and hydrocarbons. Therefore, although some ionic species, in this study, were produced during pyrolysis, the following gaseous species were specially studied: CO_2, H_2O and CH_3COOH.

Results and discussion

XRD results

The XRD patterns of original kaolinite and the kaolinite intercalated by KAc are shown in Fig.1. The $d_{(001)}$, $d_{(020)}$, $d_{(1\bar{1}0)}$, $d_{(11\bar{1})}$, $d_{(1\bar{1}1)}$ and $d_{(002)}$ diffractions of the original kaolinite are shown at 12.32, 19.84, 20.32, 21.08, 21.44 and 24.84 (2θ) with the distances of 0.715, 0.447, 0.437, 0.421, 0.414 and 0.357 nm, respectively (Fig.1a).

The XRD pattern of the original kaolinite displays a typical and well-ordered layer structure with a basal spacing (d_{001}) of 0.715 nm (Fig. 1a). These values match well with the standard ICDD reference pattern 14-0164 (kaolinite, $Al_2Si_2O_5(OH)_4$). When the kaolinite was intercalated with KAc, expansion occurred along the *C*-axis only [38]. The new peak appearing at a distance of 1.425 nm at 6.199 (2θ) (Fig.1b) signifies that the KAc molecules are directly intercalated into the kaolinite in agreement with the previous literature [39-41]. It is shown that the basal $d_{(001)}$ of kaolinite expands from 0.715 to 1.425 nm; the increment of 0.71 nm in *d*-value of kaolinite indicates the intercalation of KAc in the interlamellar space. The effect of KAc intercalation causes the intensity decrease of the $d_{(001)}$ spacing for kaolinite, and the significance of the loss of intensity for the $d_{(001)}$ peak means the stacking between the kaolinite layers is disrupted and lost. It is reported that an increase of the structural disorder caused an obvious weakening of reflections 11l and 02l (2θ between 17 and 27 °), which were replaced by a broad peak of scattering with weak modulations [42-44]. This is due to the KAc intercalation has broken the hydrogen bonding between adjacent kaolinite layers. The kaolinite intercalated with KAc causes the expansion of its layers in the c direction, and results in significant changes in the kaolinite surface properties. For example, intercalation can cause significant disordering of the kaolinite, increased surface areas and provide more surface hydroxyl, which are more readily available for chemical reactions. Moreover, the diffraction peaks belonging to the $d_{(001)}$ and $d_{(002)}$ planes of kaolinite are observed at 12.53 and 25.03 (2θ) with the distances of 0.71 and 0.35 nm, respectively, indicating

that a certain portion of kaolinite remained after the intercalation process (Fig.1b). By using the ratio of the intensity of the (001) peak after and before intercalation, a measure of the degree of intercalation may be obtained [45]. For the kaolinite intercalated by KAc with the solution concentrations of 30%, the degree of intercalation is found to be 0.87 (87% intercalated).

Thermal analysis

The thermogravimetric and differential thermogravimetric (TG-DTG) measurement of original kaolinite and kaolinite-KAc intercalation complex are performed and the results are shown in Fig. 2. Only one of main features of the DTG curves of kaolinite is the mass loss between 400 and 600 °C with a maximum rate at 520 °C that is attributed the loss of water because of the dehydroxylation of the crystal lattice, i.e. formation meta-kaolinite. This process roughly corresponds to 13.32% mass loss in the TG curve. This value is close to the theoretical value (13.9 %). By comparison with the TG-DTG curves of the original kaolinite, four mass losses are observed in the TG curve of kaolinite-KAc intercalation complex in Fig. 2b. The TG-DTG curve of the intercalation complex presented a peak at 81 °C associated with dehydration of the complex with a 1.48 % mass loss of adsorbed water. The second peak appeared at 296 °C, accompanied by a mass loss of 1.27 % caused by thermal decomposition of surface-adsorbed KAc. This will be further proved by the mass spectrometric analysis and infrared spectroscopic analysis of the evolved gases. It is well known that the kaolinite-KAc intercalation complex is formed from the expansion of kaolinite with both KAc and water molecule [46, 47]. Therefore, the

TG-DTG curves of the intercalation complex presented a mass loss of 22.88 % between 300 and 520 °C with a maximum rate at 378 °C is attributed to thermal decomposition of intercalated KAc and dehydroxylation of the intercalated kaolinite at the elevated temperature. TG-FTIR-MS studies showed that this process in the temperature between 300 and 520 °C is a complex process and that the thermal decomposition of the complex takes place in three overlapping stages. In this temperature steps, water, acetone, acetic acid, carbon dioxide are evolved which was confirmed by mass spectrometry. Further research showed that the mass loss at 378 °C for the intercalation sample corresponded to the dehydration of the kaolinite-KAc intercalation complex. This step can be interpreted as being due to the loss of intercalated water which is coordinated to KAc in the interlayer of kaolinite. The mass loss is observed in the TG-DTG curves of kaolinite-KAc intercalation at 411 °C with mass loss of 7.54 %, which is attributed to the dehydroxylation of kaolinite. It was also stated that early dehydroxylation is due to the removal of inner surface hydroxyls which are hydrogen bonded to the intercalating acetate ions, while the second step is due to the removal of hydroxyls which are not hydrogen-bonded to the acetate [48]. The mass loss of 3.02 % between 450 and 520 °C with a maximum rate at 486 °C is attributed to the loss of the inner hydroxyl. It was reported that the inner hydroxyl was not affected by intercalated KAc [49, 44]. This result is consistent with the inner hydroxyls are below the aluminum atoms and extend towards the intralayer cavity (vacant octahedral site) of the kaolinite. At higher temperatures, a broad mass loss effect (between 700 and 830 °C) in DTG curve are observed, which

154 correspond to the thermal decomposition of potassium carbonate.

155 It is pointed out that KAc molecule possessing both proton-donor and
156 proton-acceptor group is easily intercalated. The lone pair electros of the carbonyl
157 oxygen in the acetate ion are more available for hydrogen bonding than those of the
158 siloxane groups of kaolinite [50]. In KAc solution, the cation and anion begin to share
159 water molecules and the conditions become favorable for intercalation, which
160 apparently is initiated by the acetate ion. This ion is hydrogen bonded to water
161 principally through the lone pair electrons of the carbonyl groups. Therefore, the
162 intercalation reaction destroys the inherent hydrogen bond of kaolinite and presents
163 some new bonds [51], and the kaolinite-KAc intercalation complex was formed from
164 the expansion of kaolinite with both KAc and water molecule.

165

166 *Mass spectrometric analysis of the evolved gases*

167 In accordance with former findings several different steps of thermal
168 decomposition process have occurred. In order to clarify the thermal decomposition
169 mechanism of kaolinite-KAc intercalation complex and understand well the
170 dehydration of interlayer and structural water for this complex, the mass loss during
171 each decomposition process should be characterized by the identified evolution
172 components. The mass spectrometric data also provide evidence on the thermal
173 decomposition products. The evolved products during the thermal decomposition of
174 kaolinite-KAc intercalation complex were determined by thermogravimetry coupled
175 to a mass spectrometer and are shown in Fig.3. The interpretation of the mass spectra

176 occurs on the basis of degassing profiles from the molecule ions of water (H_2O:
177 m/Z=18), carbon dioxide (CO_2: m/Z=44), acetone (C_3H_6O: m/Z=58), acetic acid
178 (CH_3COOH: m/Z=60) as well as by fragment ions (CH_3^+: m/Z=15, O^+: m/Z=16, OH^+:
179 m/Z=17, $C_2H_3O^+$: m/Z=43 and $COOH^+$: m/Z=45).

180 The characterization of water release by means of mass spectra is possible with
181 the molecule ion H_2O^+ (m/Z=18) together with the fragment ion OH^+ (m/Z=17) and
182 O^+ (m/Z=16). Peaks at 81, 378 and 486 °C for the intercalation complex are found in
183 the ion current curve for H_2O^+ (m/Z=18); corresponding peaks are also found in the
184 ion current curves for OH^+ (m/Z=17) and O^+ (m/Z=16). It can be safely concluded
185 that the water is given out at about 81 °C, 378 °C and 486 °C for the kaolinite-KAc
186 intercalation complex. The evolution profiles of the ions at m/Z=60 (CH_3COOH) and
187 m/Z=45 ($COOH^+$) the fragment ion are used to identify the presence of acetic acid. A
188 small peak at 296 °C is observed in the fragment ion current curve for acetic acid
189 (m/Z=60). This observation is due to the liberation of acetic acid after potassium
190 acetate hydrolysis. The small peaks at 378 °C in the fragment ion current curves for
191 acetic acid (m/Z=60) also are observed. This is assigned to the hydrolysis of
192 intercalated KAc and water molecules. The MS data, using m/Z=58 and 43 curves, for
193 the decomposition process indicated that acetone was produced. The broad peak
194 between 350 and 600 °C with a maximum rate at 400 °C is found in the ion current
195 curve for C_3H_6O (m/Z=58). This illustrate acetone is given out in this temperature
196 range. Moreover, the peaks at 378 °C, 411 °C and 733 °C are found in the ion current
197 curve for CO_2^+ (m/Z=44). This illustrate carbon dioxide (CO_2) is given out in this

198 temperature range, and which is also due to the pyrolysis of intercalated KAc. It is
199 also observed that the relative intensity of CO_2 decrease as temperature goes up. It
200 was reported by Kristóf et al. [52] that the dehydroxylation of the kaolinite-KAc
201 complex took place at 375 °C, as indicated by the response curve of the water detector.
202 Concerning the decomposition pattern of this complex, it is interesting to note that
203 decomposition takes place in three stages at 378, 411 and 486 °C as shown by the
204 TG-DTG curves. In addition to the liberation of water, formation of carbon dioxide
205 and acetic acid, from the decomposition of the interlayer potassium acetate, was also
206 confirmed by the Infrared spectroscopy analysis of the evolved gases. It was reported
207 that the alkali salts of acetic acid decompose to K_2CO_3 along with the liberation of
208 acetone [53-55]. According to experimental results of the mass spectrometric analysis,
209 the gaseous species produced by the thermal decomposition using the mass spectra
210 made evident the following:
211 a) The evolved products at 81 °C: water;
212 b) The evolved products at 296 °C: water, acetic acid;
213 c) The evolved products at 378 °C: water, acetone, acetic acid, carbon dioxide;
214 d) The evolved products at 411, 486 °C: water, acetone, carbon dioxide;
215 e) The evolved products at 733 °C: carbon dioxide;
216 Based on these results, it is proposed that acetic acid can form in a small amount
217 at the initial step of dehydroxylation through the reaction of the acetate ion and the
218 connecting inner surface OH group (or with dehydroxylation water), and the acetate
219 ligand is decomposed to form acetone between 300-520 °C. In this temperature range,

220 water, carbon dioxide, acetone and acetic acid are evolved which is confirmed by
221 mass spectrometry. According to experimental results of thermal analysis and the
222 mass spectrometric analysis, the mass losses at 81 and 378 °C for the complex is
223 attributed to the loss of water, and the mass loss between 300 and 420 °C for the
224 complex is assigned to the liberation of water and acetone, formation of carbon
225 dioxide and acetic acid. In addition, according to the report by Makó et al., [56] the
226 thermal decomposition of kaolinite-KAc complex is divided into two steps: the first
227 step at 378 °C and, then, a slow process over a wide temperature range between 400
228 and 550 °C. It was also stated that early dehydroxylation is due to the removal of
229 inner surface hydroxyls which are hydrogen bonded to the intercalating acetate ions,
230 while the second step is due to the removal of hydroxyls which are not
231 hydrogen-bonded to the acetate. Therefore, it is concluded that the water associated
232 with KAc and Al^{3+}-OH was removed at 378 °C and then the KAc between the layers
233 of kaolinite was decomposed. The mass loss close to 411 °C was interpreted from two
234 steps: The first step is the thermal decomposition of intercalated KAc in the interlayer
235 of kaolinite. The second step is attributed to loss of inner surface hydroxyls. The water
236 released out at 486 °C is due to the loss of the inner hydroxyl. The carbon dioxide
237 released from the complex is observed at 733 °C, which is due to the thermal
238 decomposition of K_2CO_3.
239
240 *Infrared spectroscopy analysis of the evolved gases*
241 Fig.4 shows 3D FTIR spectra for the gases produced from the thermal

242 decomposition of the kaolinite-KAc intercalation complex. By comparing the spectra
243 over the range 296-733 °C, it is important to note that the spectra not only provide the
244 information about the species of the released gas, but also display the relative
245 intensities of the evolved gas. Combined with the mass spectroscopic analysis, main
246 products are identified as follows: water (H_2O), acetone (C_3H_6O) and carbon dioxide
247 (CO_2). The emission of CO_2 is confirmed by the appearance of absorption bands in
248 the range 2217-2391 cm^{-1}. The FTIR spectra of acetone and acetic acid are rather
249 similar. The most intense bands of acetone are at 1710 cm^{-1} (C=O stretch), 1420 and
250 1210 cm^{-1}. However, in the IR spectrum of acetic acid the most intense bands are at
251 1710, 1400 and 1290 cm^{-1}. Thus, the gas phase spectra are not reliable to
252 unequivocally distinguish between acetone and acetic acid. The emission of water
253 follows four steps. At low temperature, the absorbed water is released out by
254 evaporation. Furthermore, the water associated with KAc was removed at 378 °C.
255 Moreover, when the temperature reaches 411 °C, water was generated by the loss of
256 inner surface hydroxyls which are hydrogen bonded to the intercalating acetate ions.
257 At 486 °C, an amount of water released out by the loss of the inner hydroxyl for the
258 kaolinite according to the characteristic band at 3500-3850 cm^{-1}.

259 In order to follow these thermal decompositions seven spectra at 296, 378, 411,
260 486 and 733 °C were selected for further analysis. FT-IR spectra of thermal
261 decomposition products of the kaolinite-KAc intercalation complex at these
262 temperatures are shown in Fig. 5. The spectra clearly show the temperature at which
263 the water and carbon dioxide are released out and at which the complex decomposed.

At 296 °C, the spectrum in the 1394-1090 cm^{-1} range presents two bands at 1363 and 1194 cm^{-1} which is due to the stretching vibration of C-O and deformation vibrational modes of OH, and the bands observed in the 3100-2800 cm^{-1} are attributed to COOH vibrations. These are typical of the vibrational modes for acetic acid. It is reported that the symmetric deformation band of the CH_3 group is observed in the spectrum at 1340 cm^{-1} for the intercalation complex, and the symmetric stretching band of the O-C-O unit in acetate observed at 1409 cm^{-1} as a result of hydrogen-bonding with inner surface OH groups in the intercalation complex [56, 57]. At the same time, the carbon dioxide (CO_2) is still detected by the *in situ* FTIR spectroscopic evolved gas analysis. As the temperature of the system is raised, the emission of water (H_2O) mainly occurred between 300 and 411 °C, and this temperature range of mass loss is attributed to the loss of water coordinated to KAc and then the thermal decomposition of the intercalated KAc. These results agree with our previous studies [58, 59], where an increase in the rate of mass loss at 378 °C for the intercalation sample corresponded to dehydration of intercalated kaolinite along with the liberation of a small amount of acetate decomposition products. When the temperature reaches 486 °C, water was generated by the dehydroxylation of kaolinite and confirmed by the appearance of bands at 3500-3640 cm^{-1}. It is also observed that the intensities of the CO_2 and the water are higher than that of other evolved gases. This evolved process can be divided into two parts: the first evolved process for the CO_2 and the water occurred between 296 and 400 °C with the maximum rate at 378 °C, and this temperature range of losing these two types of products is attributed to thermal

decomposition of KAc; the second evolved process for the CO_2 and the water between 400 and 500 °C with a maximum at 411 °C is due to the dehydroxylation of kaolinite and thermal decomposition of surface adsorbed KAc (after melting at 292 °C). At 733 °C, an amount of CO_2 released out according to the characteristic band at 2217-2391 cm^{-1}. This is due to the thermal decomposition of K_2CO_3.

Based on the results of this study and through reviewing and summarizing various study results, it is therefore proposed that the thermal decomposition processes for kaolinite-KAc intercalation complexes is divided into five steps. The first step is thermal decomposition of surface-adsorbed KAc. The second step is loss of the water coordinated to potassium acetate in the intercalated kaolinite. The third step is attributed to the thermal decomposition of intercalated KAc in the interlayer of kaolinite. And then the inner surface hydroxyls formed water. The last step is loss of the inner hydroxyls.

Conclusions

The products evolved during the thermal decomposition of the kaolinite-KAc intercalation complex were studies by using TG-FTIR-MS technique. The main mass losses for the thermal decomposition of this complex were observed at 81, 296, 378, 411, 486 and 733 °C which were attributed to (a) loss of the adsorbed water (b) thermal decomposition of surface-adsorbed KAc (c) the loss of the water coordinated to potassium acetate in the intercalated kaolinite (d) the thermal decomposition of intercalated KAc in the interlayer of kaolinite and the removal of inner surface

hydroxyls (e) the loss of the inner hydroxyls and (f) the thermal decomposition of carbonate derived from the decomposition of KAc. It is proposed that acetic acid can form in a small amount at the initial step of dehydroxylation through the reaction of the acetate ion and the connecting inner surface OH group (or with dehydroxylation water), and the acetate ligand is decomposed to form acetone between 300-520 °C. These thermal decomposition processes and products were proved by the mass spectrometric analysis and infrared spectroscopic analysis of the evolved gases.

The main gases and volatile products released during the thermal decomposition of the kaolinite-KAc intercalation complex are water vapor (H_2O), acetone (C_3H_6O), carbon dioxide (CO_2) and acetic acid (CH_3COOH). The main evolved product H_2O is mainly released at 81°C, and the acetic acid is given out at 296 °C. Under the temperature of 300-500 °C, the main evolved products are H_2O, C_3H_6O and CO_2. The mass spectrometric analysis results are in good agreement with the infrared spectroscopic analysis the evolved gases. Thermal analysis and mass spectrometric analysis clearly show at which temperature the mass loss. Furthermore, infrared spectroscopic analyses give the evidence on the thermal decomposition products. These results make all explanation have the sufficient evidence. Therefore, thermal analysis coupled with spectroscopic gas analysis is demonstrated to be a powerful tool for the investigation of gas evolution from the thermal decomposition of materials. Using different gas analyzing methods like MS and FTIR increases the unambiguous interpretation of the results.

Acknowledgements

The authors gratefully acknowledge the financial support provided by the National Natural Science Foundation of China (No. 51034006) and the Open Research Project of State Key Laboratory for Coal Resources and Safe Mining, China University of Mining &Technology (SKLCRSM11KFB06).

References

1. Caglar B, Çırak Ç, Tabak A, Afsin B, Eren E. Covalent grafting of pyridine-2-methanol into kaolinite layers. J Mol Struct. 2013;1032:12-22.
2. Matusik J, Scholtzova E, Tunega D. Influence of synthesis condition on the formation of a kaolintie-methanol complex and simulation its vibrational spectra. Clay Clay Miner. 2012;60:227-39.
3. Caglar B. Structural characterization of kaolinite-nicotinamide intercalation composite. J Mol Struct. 2012;1020:48-55.
4. Letaief S, Leclercq J, Liu Y, Detellier C. Single kaolinite nanometer layers prepared by an in situ polymerization–exfoliation process in the presence of ionic liquids. Langmuir. 2011;27:15248-54.
5. Cheng H, Liu Q, Zhang J, Yang J, Frost RL. Delamination of kaolinite-potassium acetate intercalates by ball-milling. J Colloid Interface Sci. 2010;348:355-9.
6. Cheng H, Liu Q, Yang J, Zhang Q, Frost RL. Thermal behavior and decomposition of kaolinite-potassium acetate intercalation composite. Thermochim Acta. 2010;503-504:16-20.
7. Letaief S, Detellier C. Functionalization of the interlayer surfaces of kaolinite by alkylammonium groups from ionic liquids. Clay Clay Miner. 2009;57:638-48.
8. Letaief S, Detellier C. Clay-polymer nanocomposite material from the delamination of kaolinite in the presence of sodium polyacrylate. Langmuir. 2009;25:10975-9.
9. Pavlidou S, Papaspyrides CD. A review on polymer-layered silicate nanocomposites. Prog Polym Sci. 2008;33:1119-98.
10. Frost RL, Horváth E, Makó É, Kristóf J, Cseh T. The effect of mechanochemical activation upon the intercalation of a high-defect kaolinite with formamide. J Colloid Interface Sci. 2003;265:386-95.
11. Frost RL, Horváth E, Makó É, Kristóf J. Modification of low- and high-defect kaolinite surfaces: Implications for kaolinite mineral processing. J Colloid Interface Sci. 2004;270:337-46.
12. Gardolinski JEFC, Lagaly G. Grafted organic derivatives of kaolinite: Ii. Intercalation of primary n-alkylamines and delamination. Clay Miner. 2005;40:547-56.
13. Jia X, Li Y, Zhang B, Cheng Q, Zhang S. Preparation of poly(vinyl alcohol)/kaolinite nanocomposites via in situ polymerization. Mater Res Bull. 2008;43:611-7.
14. Franco F, Pérez-Maqueda LA, Pérez-Rodr´ıguez JL. The influence of ultrasound on the thermal behaviour of a well ordered kaolinite. Thermochim Acta. 2003;404:71-9.
15. Franco F, Pérez-Maqueda LA, Pérez-Rodríguez JL. The effect of ultrasound on the particle size and structural disorder of a well-ordered kaolinite. J Colloid Interface Sci. 2004;274:107-17.
16. Franco F, Cecila JA, Pérez-Maqueda LA, Pérez-Rodríguez JL, Gomes CSF. Particle-size reduction of dickite by ultrasound treatments: Effect on the structure, shape and particle-size distribution. Appl Clay Sci. 2007;35:119-27.
17. Churchman GJ, Whitton JS, Claridge GGC, Theng BKG. Intercalation method using formamide for differentiating halloysite from kaolinite. Clays Clay Miner. 1984;32:241-8.
18. Joussein E, Petit S, Delvaux B. Behavior of halloysite clay under formamide treatment. Appl Clay Sci. 2007;35:17-24.
19. Costanzo PM, R. F. Giese J. Ordered halloysite: Dimethylsulfoxide intercalate. Clays Clay Miner. 1986;34:105-7.
20. Nicolini KP, Fukamachi CRB, Wypych F, Mangrich AS. Dehydrated halloysite intercalated

mechanochemically with urea: Thermal behavior and structural aspects. Journal of Colloid and Interface Science. 2009;338:474-9.
21. Frost RL, Kristof J, Horvath E, Kloprogge JT. Rehydration and phase changes of potassium acetate-intercalated halloysite at 298 k. J Colloid Interface Sci. 2000;226:318-27.
22. Luca V, Thomson S. Intercalation and polymerisation of aniline within a tubular aluminosilicate J Mater Chem. 2000;10:2121-6.
23. Horváth E, Kristóf J, Frost R, Rédey Á, Vágvölgyi V, Cseh T. Hydrazine-hydrate intercalated halloysite under controlled-rate thermal analysis conditions. J Therm Anal Calorim. 2003;71:707-14.
24. Benazzouz BK, Zaoui A. Thermal behaviour and superheating temperature of kaolinite from molecular dynamics. Appl Clay Sci. 2012;58:44-51.
25. Cheng H, Liu Q, Yang J, Du X, Frost RL. Influencing factors on kaolinite-potassium acetate intercalation complexes. Appl Clay Sci. 2010;50:476-80.
26. Cheng H, Liu Q, Yang J, Ma S, Frost RL. The thermal behavior of kaolinite intercalation complexes-a review. Thermochim Acta. 2012;545:1-13.
27. Ahamad T, Alshehri SM. Tg–ftir–ms (evolved gas analysis) of bidi tobacco powder during combustion and pyrolysis. J Hazard Mater. 2012;199–200:200-8.
28. Madarász J, Brăileanu A, Crişan M, Pokol G. Comprehensive evolved gas analysis (ega) of amorphous precursors for s-doped titania by in situ tg–ftir and tg/dta–ms in air: Part 2. Precursor from thiourea and titanium(iv)-n-butoxide. J Anal Appl Pyrol. 2009;85:549-56.
29. Madarász J, Varga PP, Pokol G. Evolved gas analyses (tg/dta–ms and tg–ftir) on dehydration and pyrolysis of magnesium nitrate hexahydrate in air and nitrogen. J Anal Appl Pyrol. 2007;79:475-8.
30. Madarász J, Pokol G. Comparative evolved gas analyses on thermal degradation of thiourea by coupled tg-ftir and tg/dta-ms instruments. J Therm Anal Calorim. 2007;88:329-36.
31. Kaljuvee T, Keelman M, Trikkel A, Petkova V. Tg-ftir/ms analysis of thermal and kinetic characteristics of some coal samples. J Therm Anal Calorim. 2013;113:1063-71.
32. Cheng H, Liu Q, Zhang S, Wang S, Frost R. Evolved gas analysis of coal-derived pyrite/marcasite. J Therm Anal Calorim. 2014;116:887-94.
33. Cheng H, Liu Q, Liu J, Sun B, Kang Y, Frost R. Tg–ms–ftir (evolved gas analysis) of kaolinite–urea intercalation complex. J Therm Anal Calorim. 2014;116:195-203.
34. Fischer M, Wohlfahrt S, Saraji-Bozorgzad M, Matuschek G, Post E, Denner T, Streibel T, Zimmermann R. Thermal analysis/evolved gas analysis using single photon ionization. J Therm Anal Calorim. 2013;113:1667-73.
35. Arockiasamy A, Toghiani H, Oglesby D, Horstemeyer MF, Bouvard JL, King R. Tg–dsc–ftir–ms study of gaseous compounds evolved during thermal decomposition of styrene-butadiene rubber. J Therm Anal Calorim. 2013;111:535-42.
36. Bednarek P, Szafran M. Thermal decomposition of monosaccharides derivatives applied in ceramic gelcasting process investigated by the coupled dta/tg/ms analysis. J Therm Anal Calorim. 2012;109:773-82.
37. Cheng H, Yang J, Frost R, Liu Q, Zhang Z. Thermal analysis and infrared emission spectroscopic study of kaolinite–potassium acetate intercalate complex. J Therm Anal Calorim. 2011;103:507-13.
38. Zhang B, Li Y, Pan X, Jia X, Wang X. Intercalation of acrylic acid and sodium acrylate into kaolinite and their in situ polymerization. J Phys Chem Solids. 2007;68:135-42.
39. Franco F, Ruiz Cruz MD. Factors influencing the intercalation degree ('reactivity') of kaolin

minerals with potassium acetate, formamide, dimethylsulphoxide and hydrazine. Clay Miner. 2004;39:193-205.
40. Deng Y, White GN, Dixon JB. Effect of structural stress on the intercalation rate of kaolinite. J Colloid Interface Sci. 2002;250:379-93.
41. Frost RL, Kristof J, Paroz GN, Kloprogge JT. Role of water in the intercalation of kaolinite with hydrazine. J Colloid Interface Sci. 1998;208:216-25.
42. Hinckley DN. Variability in "crystallinity" values among the kaolin deposits of the coastal plain of georgia and south carolina. Clay Clay Miner. 1963;11:229-35.
43. Frost RL, Kristof J, Paroz GN, Kloprogge JT. Molecular structure of dimethyl sulfoxide intercalated kaolinites. J Phys Chem B. 1998;102:8519-32.
44. Frost RL, Kristof J, Tran TH. Kinetics of deintercalation of potassium acetate from kaolinite; a raman spectroscopic study. Clay Miner. 1998;33:605-17.
45. Wiewióra A, Brindley GW. Potassium acetate intercalation in kaolinites and its removal: Effect of material characteristics. In: Heller L, editor. Proceedings of the International Clay Conference Tokyo: Israel University Press, Jerusalem; 1969. p. 723-33.
46. Wada K. Lattice expansion of kaolin minerals by treatment with potassium acetate. Am Mineral. 1961;46:78-91.
47. Frost RL, Kristof J, Kloprogge JT, Horvath E. Rehydration of potassium acetate-intercalated kaolinite at 298 k. Langmuir. 2000;16:5402-8.
48. Cheng H, Liu Q, Cui X, Zhang Q, Zhang Z, Frost RL. Mechanism of dehydroxylation temperature decrease and high temperature phase transition of coal-bearing strata kaolinite intercalated by potassium acetate. J Colloid Interface Sci. 2012;376:47-56.
49. Kristof J, Frost RL, Felinger A, Mink J. Ftir spectroscopic study of intercalated kaolinite. J Mol Struct. 1997;410-411:119-22.
50. Yamuna A, Devanarayanan S, Lalithambika M. Phase-pure mullite from kaolinite. J Am Ceram Soc. 2002;85:1409-13.
51. Mellouk S, Cherifi S, Sassi M, Marouf-Khelifa K, Bengueddach A, Schott J, Khelifa A. Intercalation of halloysite from djebel debagh (algeria) and adsorption of copper ions. Appl Clay Sci. 2009;44:230-6.
52. He H, Yuan P, Guo J, Zhu J, Hu C. The influence of random defect density on the thermal stability of kaolinites. J Am Ceram Soc. 2005;88:1017-9.
53. Knopp JA, Linnell WS, Child WC. The thermodynamics of the thermal decomposition of acetic acid in the liquid phase. J Phys Chem. 1962;66:1513-6.
54. Nguyen MT, Sengupta D, Raspoet G, Vanquickenborne LG. Theoretical study of the thermal decomposition of acetic acid: Decarboxylation versus dehydration. J Phys Chem. 1995;99:11883-8.
55. Mackie JC, Doolan KR. High-temperature kinetics of thermal decomposition of acetic acid and its products. Int J Chem Kinet. 1984;16:525-41.
56. Cheng H, Liu Q, Yang J, Zhang J, Frost RL. Thermal analysis and infrared emission spectroscopic study of halloysite-potassium acetate intercalation compound. Thermochim Acta. 2010;511:124-8.
57. Cheng H, Liu Q, Yang J, Zhang J, Frost RL, Du X. Infrared spectroscopic study of halloysite-potassium acetate intercalation complex. J Mol Struct. 2011;990:21-5.
58. Frost RL, Kristof J, Mako E, Kloprogge JT. Modification of the hydroxyl surface in potassium-acetate-intercalated kaolinite between 25 and 300^{o}c. Langmuir. 2000;16:7421-8.
59. Cheng H, Yang J, Liu Q, He J, Frost RL. Thermogravimetric analysis-mass spectrometry (tg-ms) of

selected chinese kaolinites. Thermochim Acta. 2010;507-508:106-14.

LIST OF FIGURES

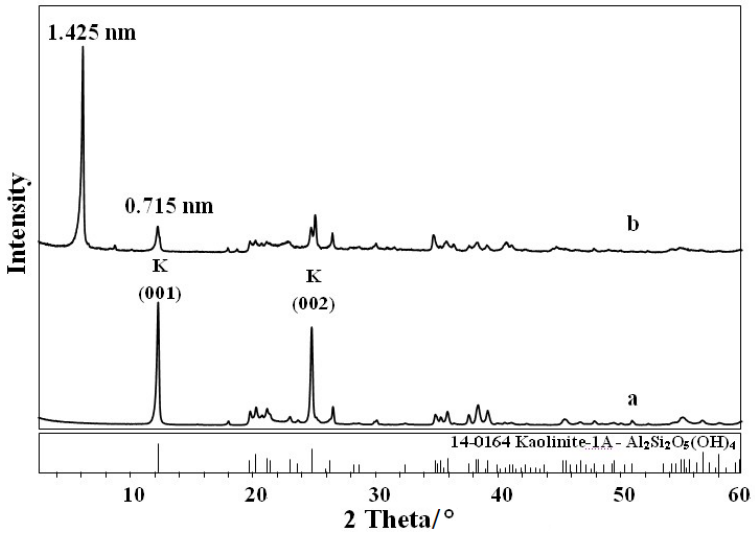
1.425 nm
0.715 nm
b
K
(001)
K
(002)
a
Intensity
14-0164 Kaolinite-1A - Al2Si2O5(OH)4
10
20
30
40
50
60
2 Theta/°

Fig.1

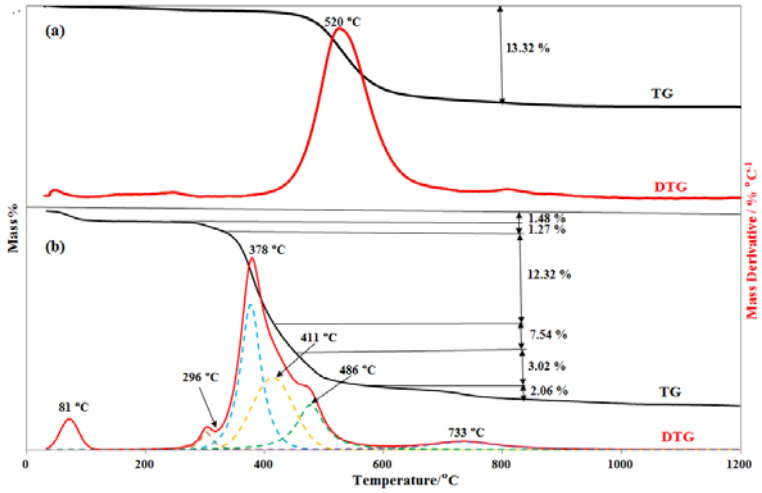
(a)
520 °C
13.32 %
TG
DTG
(b)
1.48 %
1.27 %
378 °C
12.32 %
411 °C
7.54 %
296 °C
486 °C
3.02 %
2.06 %
81 °C
733 °C
TG
DTG
Mass %
Mass Derivative / % °C-1
0
200
400
600
800
1000
1200
Temperature/°C

Fig.2

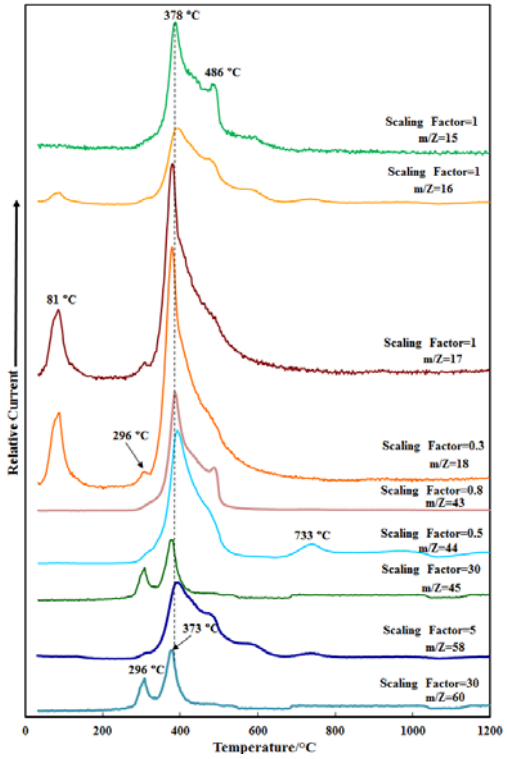
378 °C
486 °C
Scaling Factor=1
m/Z=15
Scaling Factor=1
m/Z=16
81 °C
Scaling Factor=1
m/Z=17
296 °C
Scaling Factor=0.3
m/Z=18
Scaling Factor=0.8
m/Z=43
733 °C
Scaling Factor=0.5
m/Z=44
Scaling Factor=30
m/Z=45
373 °C
Scaling Factor=5
m/Z=58
296 °C
Scaling Factor=30
m/Z=60
Relative Current
0
200
400
600
800
1000
1200
Temperature/°C

Fig.3

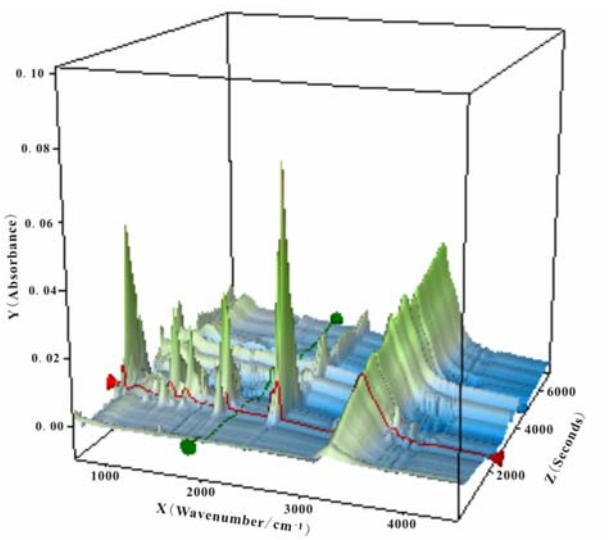
0. 10
0. 08
0. 06
0. 04
0. 02
0. 00
Y (Absorbance)
1000
2000
3000
4000
X (Wavenumber/cm-1)
2000
4000
6000
Z (Seconds)

Fig.4

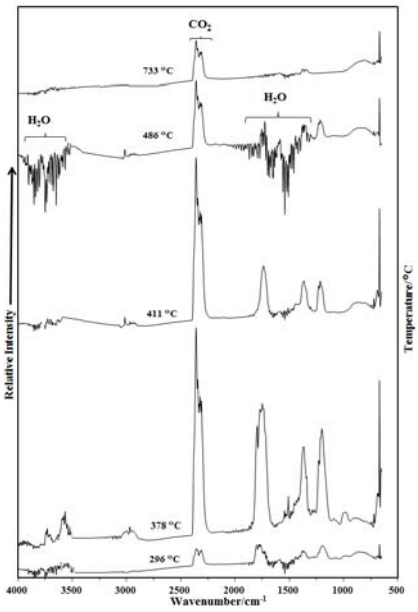
CO2
733 °C
H2O
H2O
488 °C
411 °C
378 °C
296 °C
Relative intensity
Temperature/°C
4000
3500
3000
2500
2000
1500
1000
500
Wavenumber/cm-1

Fig.5